Check-Up of Planet Earth at the Turn of the Millennium - anticipated new phase in earth sciences

Y. J. Kaufman and V. Ramanathan

Popular Summary

There is growing evidence that our climate is changing at an unprecedented rate. Some of the change is natural; some is attributed to changes in atmospheric pollution from human emissions (e.g., factories and cars). Scientists have studied climate change for the last two centuries, but the most significant progress has been made in the last 100 years. Since the revolutionary solar and lunar spectral measurements made by Langley, and Arrhenius' first estimates of the effects of greenhouse gases on climate, we have a much better understanding of how gases emitted from cars and fires can raise global temperatures. But we still do not completely understand climate; nor can we predict how it will evolve in the future without measuring the numerous rapid impacts of humans on our planet, as well as the natural changes that occur. To study how climate will change, we need to measure the concentrations of pollutants in the atmosphere, observe the changes in land and marine vegetation as temperatures change, quantify emissions from volcanic activity, etc. In short, we need to globally observe and assess how processes and parameters in the Earth's atmosphere, lands, and oceans all interact to change climatic and environmental conditions; and to distingush those trends that are natural from those that are human-induced.

Next year NASA will launch the first in a series of Earth Observing System satellites, called EOS AM-1. This satellite, and others that follow, will orbit the earth and collect data on the physical state of the planet. EOS AM-1 will enable scientists to monitor how atmosphere, lands, and oceans change every day on a global scale. Additionally, scientists will compare how these processes and parameters change over time, thereby ascertaining how they affect each other. In this sense, EOS AM-1 will repeat Langley's experiment, but for the entire planet, thus pioneering novel observations from space. Conceived in response to real environmental problems, EOS AM-1, in conjunction with other international satellite efforts, will fill a major gap in current efforts by providing information using new technologies that can revolutionize climate research. It is anticipated that EOS will inspire a new generation of climate models to assess the human impact on the environment. In this review article submitted to *Science*, we first list the series of discoveries during the last century that set the stage for EOS AM-1. Then we describe how the trillions of bits of EOS AM-1 data will take us further towards our ultimate goal of understanding how Earth's climate will evolve in the next century.

Check-Up of Planet Earth at the Turn of the Millennium - anticipated new phase in earth sciences

Y. J. Kaufman and V. Ramanathan

Sep. 1998

ABSTRACT

Langley's remarkable solar and lunar spectra collected from Mt. Whitney inspired Arrhenius to develop the first quantitative climate model in 1896. In 1999, NASA's Earth Observing AM Satellite (EOS-AM) will repeat Langley's experiment, but for the entire planet, thus pioneering calibrated spectral observations from space. Conceived in response to real environmental problems, EOS-AM, in conjunction with other international satellite efforts, will fill a major gap in current efforts by providing quantitative global data sets with a resolution of few kilometers on the physical, chemical and biological elements of the earth system. Thus, like Langley's data, EOS-AM can revolutionize climate research by inspiring a new generation of climate system models and enable us to assess the human impact on the environment.

1. Introduction

The comprehensive spectral imaging of the planet by the new observing system, raises the intriguing metaphor of a check-up for the planet with worrying signs of the impact of its most influential inhabitants - humans (1), that tripled their population just in the last century (Fig. 1). While we can only speculate on human impacts on climate, we do have a general sense of our use of the planets resources: The land - we use 40% of it, affecting its radiative, hydrological and biochemical

properties. The atmosphere - we have changed its composition, chemistry and radiative properties by increasing the concentration of natural greenhouse gases (CO_2, CH_4) at an unprecedented rate. We generated new greenhouse gases - chloroflurocarbons, CFCs, that also threaten the protective stratospheric ozone layer. We increased the concentration of pollutants, including smoke and urban/industrial "sulfate" aerosol, and changed atmospheric chemistry by increasing the harmful tropospheric ozone in polluted regions.

What is the purpose of this new observing system in space? The earth system is driven by slowly varying (greenhouse gases) and rapid processes: cloud radiative forcing, soil moisture, vegetation feedback to increased CO_2 concentration, oceanic chlorophyll variability among many others. Models that attempt to simulate climate from "first" principles, e.g. GCMs, have difficulty in accounting for the fast processes due to lack of global data, low model resolution and complexity of the physical/chemical / biological processes. For example, the simulated temperature change for the last century was about twice as large as the climate record, after accounting for the increase in concentration of greenhouse gases. By adding only the direct radiative forcing of sulfates, the discrepancy nearly "disappeared" (2). But other equally important parameters (e.g., vegetation effects, clouds, ocean heat transport) are still not properly accounted for. To fill this gap, models need high quality data to initialize and validate their performance. Some earth processes, e.g. the chemical complexity of aerosols, may be beyond the reach of models for decades to come. However, they can be directly estimate from EOS-AM and used in tandem with simpler models to assess the impact on climate.

EOS-AM is designed to perform a complete check-up of the earth through global characterization of its parameters and processes from space. Space observations have

been collected for the last two decades, but they lack the spectral bands, angular sampling and accuracy of calibration. EOS-AM, a unique tool for integrating wide array of observations from a single point in space and time, was developed to answer this need. Never flown before, EOS-AM with its 5 scientific instruments on board will for the first time:

- Measure the variability in the reflected solar energy and emitted terrestrial energy with simultaneous characterization of the interaction among biota, air pollution, water vapor and clouds that shape the radiation field.

- Deploy spaceborne observation capability in 50 tested and new spectral bands with multiangle and stereo vision to test hypotheses related to the Earth system for which we have no adequate tools, e.g. the impact of air pollution on clouds and the hydrological cycle or the impact of increase in CO_2 concentration and air temperature on the ability of land and oceanic biota to absorb CO_2 from the atmosphere.

- Map with unprecedented accuracy and spatial resolution the earth geological structure, surface vegetation, atmospheric composition and oceanic productivity as a basis for future detection of change, and to initiate climate models.

- Provide accurate records of the ocean and land temperature, simultaneously with vegetation productivity, humidity and cloudiness to assess the global impacts of climate seasonal variability such as El-Nino.

- In a short response time provide detailed measurements of hazards and their impacts - fires, volcanoes and floods.

In this article we first list the series of discoveries during the last century that set the stage for EOS and then describe how the trillions of bits of EOS-AM data can take us further towards our ultimate goal of understanding how the various components of our planet interact to maintain the environment.

2. Historical perspective

Climate and the greenhouse effect was a major research topic already in the early 19th century (3). Fourier (4) suggested in 1824, that the atmosphere behaves like the transparent glass cover of a box exposed to the sun by allowing sunlight to penetrate to the Earth's surface and retaining the longwave radiation ("obscure radiation") from the Earth's surface. By about the mid-nineteenth century, the pyrheliometric observation of Pouillet (5) and especially the ingenious laboratory experiments of Tyndall (6) demonstrated the selective spectral absorption of longwave radiation by atmospheric water vapor and CO_2.

Accurate atmospheric solar and infrared (IR) transmission observations were needed to extrapolate laboratory data to atmospheric conditions and construct greenhouse models of the atmosphere. Langley (7) invented the Bolometer radiometer to fill the void. Langley's observations enabled Arrhenius (8) to develop a model for the surface-atmosphere radiation budget and temperature change in 1896, thus initiating the **quantitative phase** of global warming research. Studies aimed at relating CO_2 variation to surface warming received significant impetus with the publication of Callendar's paper (9) in 1938, which concluded that atmospheric CO_2 concentration began increasing due to fossil fuel combustion since the 1900s, and that, this increase would warm the globe by about 0.03°C per decade.

Series of serendipitous developments significantly broadened the scope of the climate problem beyond that of CO_2.

- The discovery during the mid-1970s to mid-1980s, that there are several other greenhouse gases (e.g., CFCs, CH_4, N_2O, tropospheric Ozone) whose cumulative effect rivaled the greenhouse effect of anthropogenic CO_2, significantly enhanced the importance and the urgency of global warming (10). It also brought atmospheric chemists into the mainstream of global warming research.

- The convincing demonstration of the CO_2 increase by Keeling (11) and the GCM simulation of global warming of about 4K due to doubling of CO_2 (12), made it clear by the mid 1980s that serious policy options to regulate the increase of greenhouse gases must be explored. The global nature of the problem demanded an international consensus and the unprecedented Intergovernmental Panel on Climate Change was established in the late 1980s under the chairmanship of B. Bolin.

- The discovery during the 1970s and 80s, from chromatographic analyses of the gases trapped in east Antarctic (Vostok) ice cores, of the large CO_2 increase from about 170 ppm during the last glacial maximum (LGM) to about 260 ppm in the present Holocene provided great impetus for geochemists and paleo-climatologists to get into global warming research (13).

- Precise measurements of the seasonal cycle and the annual trend in atmospheric concentration of CO_2, beginning late 1950s, revealed that only 50%

of the anthropogenic CO_2 not taken up by the atmosphere, can be accounted for by oceanic uptake. Extra-tropical land biota is emerging as the likely candidate for the missing CO_2 (14). The large unanswered questions in the bio-geo-chemical cycling of anthropogenic CO_2 and the potential effects on marine and terrestrial biota brought chemistry and biology of marine and terrestrial environments as important disciplines of climate change.

- In the late 1970s it was suggested that a positive feedback between atmospheric circulation and the dependence of surface albedo on soil moisture, may be the fundamental cause for desertification in regions such as Sahel. Deforestation exposes the soil; the brighter soil reflects more solar radiation and the cooling of the column induces sinking motion which dries the surface and makes it even more brighter. Ecologists and those working on land surface processes including hydrology and vegetation were entrained as a result (15).

- Aerosol forcing emerged as a key climate change component causing the largest uncertainty in radiative forcing of climate (16). Anthropogenic aerosol particles from biomass burning and urban/industrial emissions scatter and absorb solar radiation and serve as cloud condensation nuclei (CCN) determining the cloud microphysics and interaction with sunlight, possibly even cloud fraction and precipitation (17). They are suspected to reduce the present global warming in a spatial pattern that may be eventually used as a fingerprint for detecting the response of the climate system to the greenhouse and aerosol effect (18). Stratospheric aerosol, from Mount Pinatubo eruption was predicted and later proven to cool the Earth (19).

- El-Nino: The anomalous warming of the central and eastern equatorial Pacific, is suspected to cause floods and soil erosion in California and droughts and fires in Africa, Indonesia, Brazil, Australia and recently Mexico and Florida. The El-Nino of 1997/98 was an important reminder that ocean-atmosphere interactions can dominate regional climate changes in ways that are not captured in current climate model scenario.

It became clear that the term "Global Warming" had to be modified to reflect the interests of the large community of geo-scientists, and a new term: " Global Change", was introduced in the late 1980s. It is in this context of a rapidly evolving field, drawing several disciplines into its fold, with each development enhancing significantly the value of the research to society, that we can understand the intellectual and political environment that helped create a big and broad program like EOS. The reluctance of the political establishments to take unpopular actions in the presence of large scientific uncertainty provided the impetus for funding a comprehensive evaluation of the Earth system.

3. EOS-AM instrumentation and objectives

EOS-AM MISSION

Provide a wide array of highly precise measurements from a single point in space that will be used for simultaneous mapping of global distribution of key land, ocean and atmospheric parameters: aerosol and their properties; clouds, their microphysics, optical and thermal 3-D structure; fires, their strength and emission of aerosol and trace gases; temperature of surface and air; trace gases; water vapor; bio-productivity of land and oceans and control by humans; snow and ice; and the

radiative forcing of these parameters. The measurements form the first comprehensive check-up of the Earth and initialize a long term precise monitoring of the health of the planet, the human impact, and climate variability. By taking these measurements simultaneously in space and time EOS-AM will enable process studies of the Earth system:

- Deforestation and land use effect on the vegetation cover, surface albedo, carbon budget, atmospheric composition and hydrological cycle.
- Urbanization effect on atmospheric composition, vegetation and hydrological cycle.
- Aerosol from urban/industrial emissions and biomass burning effect on cloud microphysics, reflectance and precipitation.
- Dust due to land use and climate variability effect on atmospheric stability and oceanic productivity.
- Land and oceanic productivity effect on atmospheric composition.
- Oceanic productivity effect on cloud properties through DMS originated aerosol.
- Cloud and water vapor role as feedback mechanism in climate change.
- Sea surface temperature seasonal variation effect on cloudiness, cloud vertical distribution, precipitation, droughts, continental vegetation, albedo, fires and dust production.

INSTRUMENTATION

The last two decades have witnessed a major revolution in the technology of detection and signal processing. EOS-AM as part of the Earth Observing System, following the recently launched TRIMM and SeaWiFS missions, takes advantage of this new technology, in parallel to advances in space observations by the ADEOS

series lead by Japan and ATSR and ENVISAT lead by Europe. EOS-AM, an American lead mission, assembled state of the art space instrumentation developed in Canada, Japan and the US with a diverse computer and software capability to analyze the data. Landsat 7 mission will be launched in a coordinated orbit with EOS-AM for an orchestrated observation of the Earth system.

EOS-AM will have an equatorial crossing time of 10:30 AM followed by a PM platform at year 2000 at 1:30 pm crossing time for a better representation of the diurnal variability. EOS-AM houses five instruments for simultaneous geolocated measurements and for intercomparison of the new measurements techniques. Due to the seasonality of climate, the measurement period should be at least a full year. However, due to the multitude of nonlinear processes, statistical requirements call for at least a 5 year observation period, a "snap-shot" in earth history.

Payload:

The five instruments represent a variable selection of spatial and spectral resolutions in order to observe the different scales of parameters and processes in the Earth system. Table 1 summarizes the instruments' key features.

What is new in EOS-AM ?

- **EOS-AM platform**: EOS-AM is the first large array of scientific instruments in space designed for comprehensive simultaneous observations of the land - ocean - troposphere. EOS-AM represents the transition from imaging the earth with semi-qualitative instruments with partial characterization and poor calibration (e.g., 15 years of AVHRR, TOMS and GOES/METEOSAT data) to scientific measurements

extensively characterized and calibrated before launch and during the flight. The moon will be used as the most stable radiometric calibration target to intercompare instruments on EOS-AM and compare them with future space instruments.

- **MODIS** is central to the mission: (i) along with CERES it will monitor the aerosol and cloud radiative forcing; (ii) with MISR the terrestrial vegetation, oceanic biota, aerosol and cloud properties; (iii) with MOPITT emissions of pollutants; and (iv) with ASTER soils, vegetation and cloud structure. MODIS will carry a new 1.37 μm channel 10-100 times more sensitive to cirrus clouds detection (Fig. 2a); 1.2 μm channel for snow structure; daily global 250 m channels for vegetation dynamics and identification of small clouds; global daily coverage with 7 solar spectral bands for mapping vegetation properties and for aerosol retrieval over ocean and land; chlorophyll fluorescence bands for estimation of oceanic productivity; unsaturated bands for fire characterization; thermal channels for 1 km resolution temperature profile, cloud top temperature and 2 level water vapor; near-IR bands for direct measurements of total precipitable water vapor; two mid-IR channels for cloud droplet size.

- **CERES**: combination of a cross track scanner and rotating base radiometer to characterize wide range of view angles for precise cloud radiative forcing and energy balance in the solar and IR parts of the spectrum.

- **MISR**: Simultaneous nine angle views at 270 m to 1 km for characterization of surface cover (Fig. 2c), aerosol and clouds at four spectral channels (λ<0.9 μm); stereo vision for height identification.

- **MOPITT**: first global CO maps in three layers with high spatial resolution of 22 km, first global CH_4 maps with same spatial resolution.

- **ASTER**: Thermal channels used together with visible and near-IR channels, designed for high resolution (15-90 m) stereo vision of geological features (Fig. 2b).

4. The role of EOS-AM in climate research

During the last two decades space observations have been used to provide new insights into several outstanding climate issues. We will describe EOS' role in climate research in the context of the past accomplishments.

- Land and ocean productivity feedback: The 7 PgC emitted from fossil fuel combustion and biomass burning represents only 4% of gross productivity of terrestrial vegetation and oceans (20). Even small natural or anthropogenic changes in the highly variable vegetation productivity, are likely to have a large impact on atmospheric CO_2 (14). Global measurements of the land and oceanic chlorophyll productivity are strong indicators of such changes. Satellites were used to measure vegetation "greenness" indexes over land and ocean. The index correlates with the rate of absorption of photosynthetic radiation, and with the net primary production (21). The small ratio between man-made emissions and gross productivity, leaves large room for land and ocean to mitigate or enhance the man-made imbalance in the carbon cycle in the presence of human impact on surface cover and climate change. The required high spatial resolution and accuracy to assess this delicate balance, will be provided by EOS-AM: After correction for cirrus clouds (22) and aerosol effects (23) using the new MODIS and MISR capability, the MODIS 250 m resolution channels will be used for

detection of abrupt, daily changes in the vegetation cover (24). Once detected EOS-AM will "zoom in" on the change using 15-90 m resolution ASTER and Landsat data, to map them. MODIS multispectral data, and MISR multi angular data will be used to document the spectral optical properties of the change (25), to derive global vegetation classification, surface albedo and global net primary productivity. To determine the possible causes of the change, e.g. drought or deforestation, MODIS clouds and surface temperature data will be used to correlate the land cover change with climate variability. CERES will document the effects of the changes on the atmospheric radiation budget and MOPITT on the atmospheric trace gas composition. The long term measurements will document gradual changes in the vegetation component of the carbon cycle (14, 21).

- Cloud Forcing: The Earth Radiation Budget Experiment (ERBE) yielded the first onboard calibrated radiation budget data. ERBE settled an outstanding issue by demonstrating (26) that clouds caused a large net radiative cooling of the planet. In parallel, a comprehensive study (27) that compared 19 GCMs revealed large differences in climate model predictions of cloud feedbacks in GCMs. These developments confirmed that cloud feedback is a Gordian Knot of the climate prediction problem (26). The next important step is to obtain high resolution and calibrated measurements of cloud properties, simultaneously with measurement of their radiative forcing for individual cloud systems as opposed to the traditional approach of Eulerian averages. A reconstruction of cloud three dimensional spatial structure, microphysics, radiative properties and forcing will be attempted using MODIS, MISR and CERES. MODIS will determine the daily cloud fraction using its unique spectral and spatial channels. A test of this new concept, using present satellites have been undertaken (28) with very

encouraging results (Fig. 3). With the 3-D clouds derived from the MODIS and MISR data and "zoomed in" by ASTER, we can use Monte-Carlo style radiative transfer schemes to generate cloud forcing and radiative fluxes, which will then be validated with CERES radiation data. Such 3-D reconstruction of clouds and aerosols in them will finally enable us to understand the radiative forcing and heating of realistic cloud systems, that will be used to improve climate models. EOS-AM will also measure precipitable water vapor, surface and air temperature - the main ingredients to understand the effect of seasonal and interannual variability on cloud properties.

- Atmospheric Water Vapor Greenhouse Effect: ERBE also enabled us to determine the atmospheric column greenhouse effect, Ga, for the first time. The radiative forcing due to greenhouse gases, is defined as the reduction in the outgoing longwave radiation (OLR) to space by the atmospheric gases. ERBE determined the clear sky OLR, and correlative data for surface temperatures and surface emissivity yields the surface emission. The difference between the two is g_a, which is shown globally in Fig. 4, along with water vapor. Clearly there is a strong similarity between Ga and water vapor, which demonstrates the role of water vapor in regulating the atmospheric greenhouse effect. CERES on EOS-AM, along with MODIS observations of water vapor will enable us to unravel the dominant role of water vapor greenhouse effect in climate.

- Aerosol Forcing: Satellites were used for semi-quantitative global monitoring of aerosol distribution in one or two spectral channels (29). Aerosol has a distinct spectral signature as demonstrated for the case of smoke in Fig. 5. Accurate spectral satellite data are required to measure the highly variable aerosol radiative forcing (30). Analysis of AVHRR data over the South American

biomass burning region shows that satellites can be used to measure the aerosol effect on cloud droplet size and reflectance. In this case the smoke has only a small radiative forcing due to the low cloud fraction during the dry season (14). But if a small fraction of the smoke is transported to oceanic regions with low natural CCN concentrations (31), and higher cloud fraction, the indirect forcing can be substantial (of the order of $-1 W/m^2$). Sulfate aerosol can have a similar effect on clouds and climate (16). But uncertainty in these estimates is about factor of 4. Thus the aerosol-cloud interaction can wipe out present greenhouse warming or be of marginal importance. EOS-AM together with ground based remote (32) and in situ (33) measurements and with models of the aerosol evolution will be used to reduce the uncertainty: Aerosol loading and properties will be derived using independent techniques applied to MODIS and MISR. A large array of ground based AErosol RObotic NETwork (AERONET) of autonomous radiometers will be used to evaluate and complement the spaceborne information (32,34,35). While MODIS uses daily coverage and wide spectral range to monitor aerosol, their transport and interaction with clouds, MISR observes aerosol simultaneously in several view directions, deriving their angular scattering properties. A combination of aerosol and cloud measurements by MODIS and MISR and regional flux measurements by CERES, when combined with aerosol evolution models can be the recipe for reducing the uncertainty in the aerosol forcing.

- Biomass burning for land clearing involves changes in the surface cover, narrow fire fronts and generation of burn scars that are later on replaced with less dense vegetation. The fires emit plumes of smoke particles and trace gases that eventually cover millions of square kms. Burn scars (36) will be detected by MODIS and MISR 250 m data and zoomed at with ASTER and Landsat. Fires are

measured by MODIS (37), smoke plumes by MISR and MODIS, trace gases (CO and CH4) by MOPITT and the effects on the radiation budget by CERES (26).

- Expansion of urbanization will be detected by the 250 m MODIS, and MISR data and zoomed at with ASTER and Landsat. The heat island effect of cities can be detected by MODIS and CERES, emitted aerosol plumes by MISR and MODIS, CO by MOPITT and the effects on the radiation budget by CERES. Effects of the city and its air pollution on vegetation productivity in the surrounding regions can be detected by MODIS and MISR.

- Ocean productivity, dust and climate change There is increasing evidence of the need to understand the productivity of the phytoplankton in the ocean within the framework of the complete Earth System. Productivity of the oceanic phytoplankton is the beginning of the food chain in the ocean, but it is also the main sink for atmospheric CO_2, due to accumulation during the millenniums of dead phytoplankton on the ocean floor. Therefore factors that determine its productivity are very important. The productivity of the phytoplankton is controlled by the availability of nutrients and sunlight but it is not fully understood. El-Nino, by reducing the circulation of the water in the Pacific is known for a century to reduce phytoplankton activity and fishery by reducing supply of nitrates to the surface water. But in several locations despite high nitrate concentrations the phytoplankton activity is low and iron supply from dust transported from the desert and man-made land disturbances emerges as a major factor (38). These studies required MODIS data on the oceanic phytoplankton distribution and properties, corrected for aerosol and cirrus cloud effects (22,23), accurate monitoring of the severity of dust (MODIS, MISR and

AERONET), and accurate studies of cloudiness (MODIS and MISR), and radiation budgets (CERES).

6. Conclusions

Like a person that goes for an annual health check-up somewhat belatedly during adulthood, our planet will begin the process now. Analogous to modern day diagnostics of three-dimensional imaging of the body in various electromagnetic wavelengths, EOS-AM and other international satellites will spectrally image three-dimensional structure of the planet. Advances in theory and in-situ observations will enable us to convert the spectral images in terms of environmental parameters, including: the distribution of pollution in the air, land and ocean; the fraction of natural undisturbed biota; the fraction that is influenced by humans; the interactions between atmosphere, land and oceans. The resulting data, when integrated with ongoing in-situ data collection over the oceans, cryosphere, land and atmosphere, will propel the field in two major directions.

• Modern day coupled ocean-atmosphere models have begun to incorporate the physics, chemistry, biology and dynamics of the coupled land-ocean-atmosphere system at a resolution of 50 to 100 km. It is not inconceivable that, with the advance of parallel processor computer technology, the resolution will be fine enough ($\approx$ 10 km) to resolve coastlines, mountain ranges, and most cloud systems and circulation and currents in the ocean. The primary tool for initialization and evaluation of these models will be the EOS-AM data integrated with other measurements. Some of the Earth processes may be found to be too complex to be modeled and an attempt will be made to measure and parametrize them from EOS-AM.

- We will be able to assess the human impact more accurately, by analyzing EOS-AM data in conjunction with longer term ground based measurements and field experiments; in particular the anthropogenic forcing of climate from smoke aerosols, urban pollution, land disturbance, cloud and water vapor greenhouse effect variability. With an accurate estimate of present day anthropogenic forcing, we should be able to derive the cumulative change for the last 100 years, and use it as input for climate model forecast and compare with the change in the recorded temperature record.

As a note of caution, currently there is a lack of a concerted effort at integrating the various global data sets with EOS-AM data. Such integration is necessary to distill the needed understanding from this formidable data set of over several trillion bits. It is a challenge for us to maintain and use this data record wisely and answer in a much broader sense, the question posed by Arrhenius a century ago: "*Is the mean temperature of the ground in any way influenced by the presence of the heat-absorbing gases in the atmosphere?*

References

1. P.M. Vitousek, *et al.*, *Science*, **277**, 494 (1997).
2. J.F.B. Mitchell, T.J. Johns, J.M. Gregory, and S.F.B. Tett, *Nature*, **376**, 501 (1995).
3. See excerpts of notes from Arrhenius talk in H. Rodhe, R. Charlson and E. Crawford, *Ambio*, **26**, 2-5 (1997); E. Crawford, *Ambio*, **26**, 6-11 (1997).
4. J.B. Fourier, *Mem. Acad. Sci. Inst. Fr.* **7**, 569 (1824).
5. C. Pouillet, *C.R. Aca. Sci.*, **7**, 24 (1837).
6. J. Tyndall, *Heat considered as a mode Rof motion* , 2nd ed., Longmans Green and Co., London (1865).
7. S. Langley, *Mem. Nat. Acad. Sci.*, **4**, Part II 107 (1889)

8. S. Arrhenius, *Philosophical Magazine*, **41**, 237 (1896).

9. G.S. Callendar, Q.J.R. Meteorol. Soc. **64**, 223 (1938).

10. V. Ramanathan, *Science* **190**, 50 (1975); V. Ramanathan, R.J. Cicerone, H.B. Singh and J.T. Kiehl, *J. Geophys. Res.* , **90**, 5547 (1985); V. Ramanathan, *Science*, **240**, 293 (1988).

11. C.D. Keeling, *Tellus*, **12**, 200 (1960).

12. S. Manabe and R.T. Wetherald, *J. Atmos. Sci.* **32**, 3 (1975); J.E. Hansen, A. Lacis, D. Rind, G. Russel, P. Stone, I. Fung, R. Ruedy, and J. Lerner, in: *Climate Processes and Climate Sensitivity*, Series **5**, Clark, W.C. (ed.) pp. 284. New York: Clarendon Press (1984).

13. J.M. Barnola, D. Raynaud, Y.S. Korotkevitch and C. Lorius, *Nature*, **329**, 408 (1987).

14. B.H. Braswell, D.S., Schimel, E. Linder, B.Moore, *Science*, **278**, 870 (1997); R.B. Myneni, C.D. Keeling C.J. Tucker, G. Asrar, R.R. Nemani, *Nature*, **386**, 698 (1997); C.J.Tucker, I.Y. Fung, C.D. Keeling and R.H. Gammon, *Nature*, **319**, 195 (1986); C.D. Keeling, J.F.S. Chin and T.P. Whorf, *Nature*, **277**, 146 (1996).

15. D. Skole, and C. J. Tucker, *Science*, **260**, 1905, (1993); C.J. Tucker , H.E. Dregne and W. Necomb, *Science*, **253**, 299 (1991); C.A. Nobre, P. J. Sellers, J. Shukla, Journal of Climate, **4**, 957(1991); J. Shukla, Nobre C, Sellers P., *Science*, **247**, 1322(1990); R. Kerr, *Science*, **281**, 633, (1998).

16. S.A.Twomey, M. Piepgrass and T.L. Wolfe, Tellus **36b,** 356 (1984); R.J. Charlson, S.E. Schwartz, J.M. Hales, R.D. Cess, J.A. Coakley, Jr., J.E. Hansen and D.J. Hofman, *Science*, **255**, 423 (1992).

17. Y. J. Kaufman and R. S. Fraser, *Science* **277**, 1636 (1997); Y.J. Kaufman and T. Nakajima, *J. Appl. Meteor.*, **32,** 729 (1993); Albrecht, B.A., *Science*, **245,** 1227, 1989.

18. B.D. Santer, K.E. Taylor, T.M.L. Wigley, T.C. Johns, P.D. Jones, D.J. Karoly, J.F.B. Mitchell, A.H. Oort, J.E. Penner, V. Ramaswamy, M.D. Scwarzkopf, R.J. Stouffer and S. Tett, *Nature*, **382**, 39 (1996).

19. J.E. Hansen, A. Lacis, R. Ruedy, and M. Sato, *J. Geophys. Res. Let.* **19**, 215 (1992); J.E. Hansen, A. Lacis, R. Ruedy, M. Sato, and H. Wilson, *Nat. Geog. Res. and Expl.* **9**, 142 (1993).

20. B. Bolin, *Science*, **196**, 613 (1977); P.P. Tans, I.Y. Fung and T. Takahashi, *Science*, **247**, 1431 (1990); E.T. Sunquist, *Science*, **259**, 934 (1993).

21. C.J. Tucker, J.H. Elgin Jr., and J.E. McMurtrey III, *Photogrammetric Eng. and Rem. Sens.*, **45**, 643 (1979); G. Asrar, M. Fuchs, E.T. Kanemasu and J.L. Hatfield, *Agronomy Journal* **76**, 300 (1984); P.J. Sellers, *Int. J. Rem. Sens.* **6**, 1335 (1985); S.N. Goward, C.J. Tucker and D.G. *Vegetatio*, **64**, 3 (1985).

22. B.-C. Gao and Y. J. Kaufman, *J. Atmos. Sci*, **52**, 4231 (1996).

23. Vermote, E. F., N. El Saleous, C. O. Justice, Y. J. Kaufman, J. L. Privette, L. Remer, J. C. Roger, and D. Tanré, JGR-*Atmosphere*, **102**, 17131, 1997.

24. J.G.R. Townshend & C.O. Justice, *Int. J. Rem. Sens.* **9**, 187 (1988). S.W. Running, T.R. Loveland, L.L. Pierce, R. Nemani and E.R. Hunt Jr., *Rem. Sens. Environ.* **51**, 39 (1995).

25. J. V. Martonchik, *J. Geophys. Res.* **102**, 17015 (1997); H. R. Gordon, and M. Wang, *Appl. Opt.*, **33**, 44 (1994).

26. V. Ramanathan, R.D. Cess, E.F. Harrison, P. Minnis, B.R. Barkstrom, E. Ahmad and D. Hartmann, *Science*, **243**, 57 (1989); B.A. Wielicki, B.R. Barkstrom, E.F. Harrison, R.B.L. Lee III, G.L. Smith and J. E. Cooper, *Bull., Amer. Met. Soc.*, **77**, 8853 (1996).

27. Cess RD, Potter GL, Blanchet JP, Boer GJ, Delgenio AD, Deque M, Dymnikov V, Galin V, Gates WL, Ghan SJ, Kiehl JT, Lacis AA, Letreut H, Li ZX, Liang XZ, Mcavaney BJ, Meleshko VP, Mitchell JFB, Morcrette JJ, Randall DA, Rikus L,

Roeckner E, Royer JF, Schlese U, Sheinin DA, Slingo A, Sokolov AP, Taylor KE, Washington WM, Wetherald RT, Yagai I, Zhang MH, *J. Geoph. Res.95,* 16601 (1990).

28. Boer and V. Ramanthan, in preparation, 1998

29. R. B. Husar, J. Prospero and L.L. Stowe, *J. Geophys. Res.* **102**, 16,889 (1997); J.R. Herman, P.K. Barthia, O. Torres, C. Hsu, C. Seftor, and E. Celarier, *J. Geophys. Res.* **102**, 16911 (1997).

30. C. Liousse, J.E. Penner, C. Chuang, J.J. Walton, H. Eddleman, H. Cachier, *J. Geophys. Res.*, **101**, 19411 (1996); I. Tegen, A.A. Lacis and I. Fung, *Nature*, **380**, 419 (1996). J.T. Kiehl, and B.P. Briegleb, *Science*, **260**, 311 (1993); O. Boucher and T.L. Anderson, *J. Geophys. Res.*, **100**, 26117 (1995).

31. R. Boers, G.P. Ayers and J.L. Gras, *Tellus*, **46B,** 123 (1994).

32. T. Nakajima, M. Tanaka and T. Yamauchi, *Appl. Opt.*, **22**, 2951 (1983); B.N. Holben, A. Setzer, T.F. Eck, A. Pereira and I. Slutsker, *J. Geophys. Res.* **101,** 19455 (1996).

33. J. H. Seinfeld, R. Charlson, P. A. Durkee, D. Hegg, B. J. Huebert, J. Kiehl, M. P. McCormick, J. A. Ogren, J. E. Penner, V. Ramaswamy, and W.G.N. Slinn, Aerosol radiative forcing and climate change, a plan for research, *National Academy Press*, Washington D.C. (1996); Prospero, J. M., and R. T. Nees, *Nature*, **320**, 735 (1986); J. A. Lindesay, M. O. Andreae, J. G. Goldammer, G. Hariss, H. J. Annegarn, M. Garstang, R. J. Scholes, and B. W. van Wilgen, *J. Geophys. Res.*, **101,** 23,521 (1996).

34. M. D. King, Y. J. Kaufman, P. Menzel and D. Tanré, *IEEE J. Geosci. and Rem. Sens.*, **30**, 2, (1992). D. Tanré, Y.J. Kaufman, M. Herman and S. Mattoo, *J. Geophys. Res.* , **102**, 16971 (1997); Y.J. Kaufman, D. Tanré, L. Remer, E. Vermote, A. Chu, and B.N. Holben, *J. Geophys. Res.* , **102**, 17051 (1997).

35. O. Dubovik, B.N. Holben, Y. Kaufman, M. Yamasoe, A. Smirnov, D. Tanre, I. Slutsker, submitted to *J. Geophys. Res.* (1998); M. A. Yamasoe, Y. J. Kaufman, B. Holben, P. Artaxo, submitted to *J. Geophys. Res.*. (1998); M. Wendisch and W. von Hoyningen-Huene, *Atmos. Environ.*, **28**, 785 (1994).

36. C.O. Justice, J.D.Kendall, P.R.Dowty and R.J.Scholes, *J. Geophys. Research* , **101** 23851 (1996); R.J. Scholes, D Ward and C.O. Justice, *J. Geophys. Research*, **101**, 23677 (1996).

37. Y. J. Kaufman, C. J. Tucker and I. Fung, *J. Geophys. Res.*, **95**, 9927 (1990); Y. J. Kaufman, C. Justice, L. Flynn, J. Kandall, E. Prins, D. E. Ward, P. Menzel and A. Setzer, accepted to *J. Geophys. Res.* (1998).

38. K.H. Coale, S.E. Fitzwater, R. M. Gordon, K.S. Johnson, and R.T. Barber, *Nature*, **379**, 621 (1996); Z. S. Kolber , R. T. Barber , K. H. Coale , S. E. Fitzwater , R. M. Greene, K. S. Johnson, S. Lindley, P. G. Falkowski, *Nature, 371*, 145 (1994); J. H. Martin, S. E. Fitzwater, *Nature*, **331**, 341 (1988); J. M. Prospero, K. Barrett, T. Church, F. Dentener, R. A. Duce, J. N. Galloway , H. Levy, J. Moody, P. Quinn **35**, 27 (1996).

39. D. J. Diner, L. M. Barge, C. J. Bruegge, T. G. Chrien, J. E. Conel, M. L. Eastwood, J. D. Garcia, M. A. Hernandez, C. G. Kurzweil, W. C. Ledeboer, N. D. Pignatano, C. M. Sarture, and B. G. Smith, IEEE Trans. Geosci. Rem. Sens. **36**, 1339 (1998).

40. A.K. Inamdar and V. Ramanthan, EOS *J. Geophys. Res.* special issue in print (1998).

41. We would like to thank Didier Tanre from CNRS, Jeff Kiehl from NCAR, Jim Collatz and Lorraine Remer from NASA/GSFC and Pinhas Alpert from Tel-Aviv University for valuable comments.

Figure legends:

Fig. 1: Exponential increase in the world population growth in the last 400 years, and the corresponding change in the emission of CO_2 and sulfur.

Fig 2: (a) AVIRIS simulation of the MODIS new 1.375 μm cirrus channel (22). Top - image of an ocean-land region at 0.66 μm indicating the presence of thin clouds. middle - same image at 1.375 μm, observing high clouds only, due to the strong water vapor absorption in the lower troposphere in this channel. Bottom image is the same as in top but corrected for the cirrus effect.
(b): Aircraft simulation of an ASTER image of Death Valley, California, 60 x 60 km. This image is draped over digital elevation data to produce the 3-D perspective view that will be available from ASTER (A. Kahle, personal communication). Top: visible, middle infrared and short wavelength infrared bands used for the color display of the surface composition: green - vegetation; blue - wet or standing water; orange - iron-rich volcanic rocks; brown, pink, blue gray - volcanic and sedimentary rocks. Bottom: multispectral thermal infrared bands for new surface composition and more accurate surface temperature determinations. red - quartz-rich outcrops and alluvial fans; dark green, gray, and blue - other volcanic and sedimentary rock types; light green - salt deposits on the valley floor.
(c) Color composite images taken by the AirMISR instrument on August 25, 1997 of the area surrounding Moffett Field, California (39) covering an area of 10 km on a side, acquired from NASA ER-2 aircraft at 20 kms altitude. The imaged area straddles the waters of San Francisco Bay near the inlet of Coyote Creek, mudflats, marshes, tidelands that are in part utilized as salt evaporation ponds, and urban areas of Mountain View, Sunnyvale. North is toward the top

of these images, and the sun is shining roughly from the south. For the left image, the camera was pointing at 26° forward of nadir, whereas the right image was taken with the camera pointing 26° aftward of nadir. The rivers and tidal areas are brighter in the forward-viewing (left) image, illustrating that these wet surfaces produce mirror-like reflections that are observable at this viewing geometry.

Fig. 3: Three-dimensional (3-D) reconstruction of cloud systems over the western Tropical Pacific ocean from AVHRR satellite images. The visible reflectances, in combination with in-situ microphysics data were used to obtain cloud thickness. The infrared radiances over cloud centers were used to get cloud top heights. A detection and spread algorithm (28) was used to demarcate cloud boundaries. Altitude of thin clouds are assumed to be the same as that of neighboring or attached thick clouds. The accuracy of the 3-D reconstruction shown here can be improved significantly with the MODIS channels, in particular the cirrus unmasking technique shown earlier in the text.

Fig. 4: Comparison between global observations of atmospheric greenhouse effect, g_a, (top panel) and total precipitable water vapor (lower panel). g_a is the reduction in the outgoing longwave radiation (OLR) due to the atmospheric greenhouse gases. It is derived from the difference between the OLR and the surface emitted radiation. The later is computed using correlative data of surface temperature and emissivity (40).

Fig. 5: Fig. 5: Large fire near Cuiaba on Aug. 25, 1995 taken from the ER-2 AVIRIS instrument (identified by from Robert Green from JPL) during the SCAR-B experiment. The image is 10x20 km and 20 m resolution. Top image - heavy

smoke emitted from the fire and flowing over Cuiaba. It resembles human vision and is composed of 0.47 μm (blue), 0.55 μm (green) and 0.66 μm (red). Bottom image - is for 2.1 μm (blue), 1.2 μm (green) and 1.65 μm (red). The smoke is almost transparent in these longer wavelengths and the fire is clearly seen with its 3 main temperatures zones (blue - glowing, purple - smoldering - emitting the heavy smoke, and white - the fire front). It is much easier to observe the surface features in the long wavelengths that penetrates the smoke. The solar zenith angle is 36°. The background optical thickness was 0.16 at 0.65 μm. The smoke optical thickness is on average higher by 0.6 from background, reflecting an additional 43 w/m^2 of solar radiation back to space.

Table 1: summary of the main characteristics of the 5 instruments on board EOSAMS

Instrument	ASTER	MODIS	MISR	CERES	MOPITT
Spatial resolution at nadir	15 m in visible, 30 m in the mid-IR 90 m in the IR	250 m (2 bands), 500 m (5 bands, 1000 m (29 bands)	250 m to 1 km	20 km	22 km
Spectral range	0.5-12 μm	36 bands: 0.4-14 μm	4 bands: 443, 555, 670, 865 nm	3 bands: Solar: 0.3-5.0 μm Thermal: 8-12 μm Total: 0.3 to >200 μm	3 bands: 2.3 μm (CH_4), 2.4 μm (CO), and 4.7 μm (CO)
spatial coverage **repeatability**	60 km images acquired by order	2330 km daily except near the equator	360 km 6-9 days	2330 km ? daily	640 km 3-4 days
Stereo capability	YES	NO	YES	not relevant	NO
Main measurements	geological rock and soil cover, high resolution imagery:	general land, ocean and atmospheric global studies across the solar and thermal spectrum	Application of multiview imaging for land atmospheric and ocean studies	solar, thermal and total radiation budget, cloud net radiative forcing	Global CO and CH_4 distribution
main products	• Measure spectral radiances and reflectances of the Earth's surface • Measure surface temperature and emissivities • Derive digital elevation maps from stereo images • Determine surface composition and vegetation maps • Measure cloud, sea ice, and polar ice properties • Observations of natural hazards (volcanoes, etc.)	• Measure surface temperature (land and ocean) • Measure ocean color (sediment, phytoplankton) • Derive global vegetation maps and monitor change • Measure cloud characteristics • Measure aerosol concentrations and properties • Measure temperature and moisture profiles • Measure snow cover and characteristics • Measure ocean currents	• Measure cloud angular reflectance and effect on the planetary solar radiation budget • Measure tropospheric aerosols concentration and effect on the solar radiation budget • Study angular properties of surface reflectance and the impact of land processes on climate	• Measure cloud radiative forcing and feedbacks • Derive observational baseline of clear-sky radiative fluxes	• Measure carbon monoxide and methane concentrations in the troposphere • Obtain carbon monoxide profiles with a resolution of 22 km horizontally and 3 km vertically with an accuracy of 10 % • Measure the methane column in the troposphere with a resolution of 22 km and a precision of better than 1 %
web address	.....	.....	.....	.....	.....

Cover picture: An artist's rendering of EOS-AM

Here, MODIS is illustrated collecting Normalized Difference Vegetation Index and sea surface temperature data.

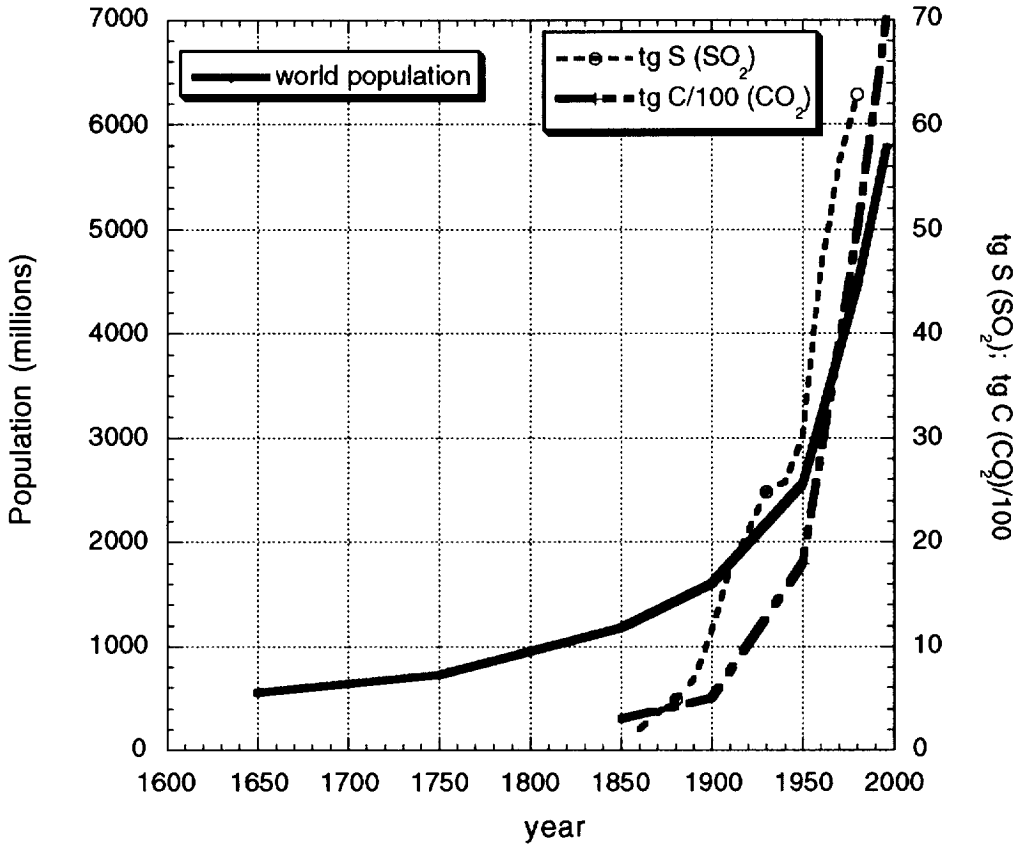

Fig. 1: Exponential increase in the world population growth in the last 400 years, and the corresponding change in the emission of CO_2 and sulfur.

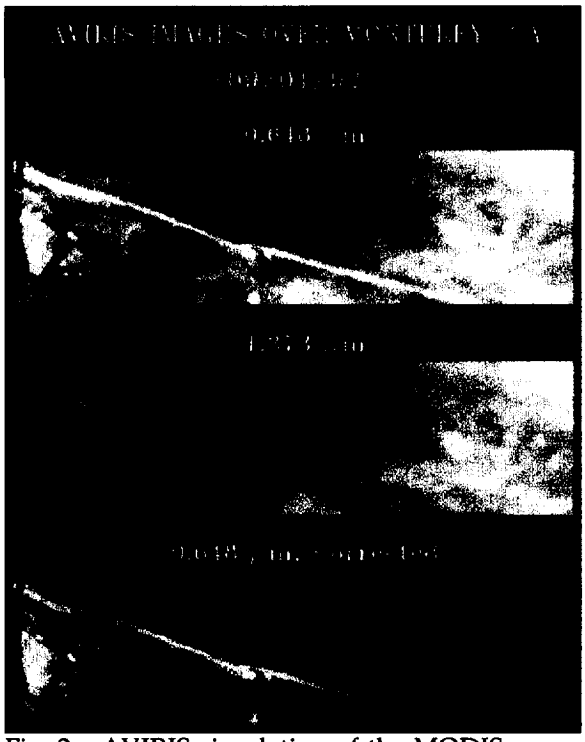

Fig. 2a: AVIRIS simulation of the MODIS new 1.375 μm cirrus channel (22). Top - image of an ocean-land region at 0.66 μm indicating the presence of thin clouds. middle - same image at 1.375 μm, observing high clouds only, due to the strong water vapor absorption in the lower troposphere in this channel. Bottom image is the same as in top but corrected for the cirrus effect.

Fig 2b: Aircraft simulation of an ASTER image of Death Valley, California, 60 x 60 km. This image is draped over digital elevation data to produce the 3-D perspective view that will be available from ASTER (A. Kahle, personal communication). Top: visible, middle infrared and short wavelength infrared bands used for the color display of the surface composition: green - vegetation; blue - wet or standing water; orange - iron-rich volcanic rocks; brown, pink, blue gray - volcanic and sedimentary rocks. Bottom: multispectral thermal infrared bands for new surface composition and more accurate surface temperature determinations. red - quartz-rich outcrops and alluvial fans; dark green, gray, and blue - other volcanic and sedimentary rock types; light green - salt deposits on the valley floor.

Fig. 2c: Color composite images taken by the AirMISR instrument on August 25, 1997 of the area surrounding Moffett Field, California (39) covering an area of 10 km on a side, acquired from NASA ER-2 aircraft at 20 kms altitude. The imaged area straddles the waters of San Francisco Bay near the inlet of Coyote Creek, mudflats, marshes, tidelands that are in part utilized as salt evaporation ponds, and urban areas of Mountain View, Sunnyvale. North is toward the top of these images, and the sun is shining roughly from the south. For the left image, the camera was pointing at 26° forward of nadir, whereas the right image was taken with the camera pointing 26° aftward of nadir. The rivers and tidal areas are brighter in the forward-viewing (left) image, illustrating that these wet surfaces produce mirror-like reflections that are observable at this viewing geometry.

Fig. 3: Three-dimensional (3-D) reconstruction of cloud systems over the western Tropical Pacific ocean from AVHRR satellite images. The visible reflectances, in combination with in-situ microphysics data were used to obtain cloud thickness. The infrared radiances over cloud centers were used to get cloud top heights. A detection and spread algorithm (28) was used to demarcate cloud boundaries. Altitude of thin clouds are assumed to be the same as that of neighboring or attached thick clouds. The accuracy of the 3-D reconstruction shown here can be improved significantly with the MODIS channels, in particular the cirrus unmasking technique shown earlier in the text.

Fig. 3: Three-dimensional (3-D) reconstruction of cloud systems over the western Tropical Pacific ocean from AVHRR satellite images. The visible reflectances, in combination with in-situ microphysics data were used to obtain cloud thickness. The infrared radiances over cloud centers were used to get cloud top heights. A detection and spread algorithm (28) was used to demarcate cloud boundaries. Altitude of thin clouds are assumed to be the same as that of neighboring or attached thick clouds. The accuracy of the 3-D reconstruction shown here can be improved significantly with the MODIS channels, in particular the cirrus unmasking technique shown earlier in the text.

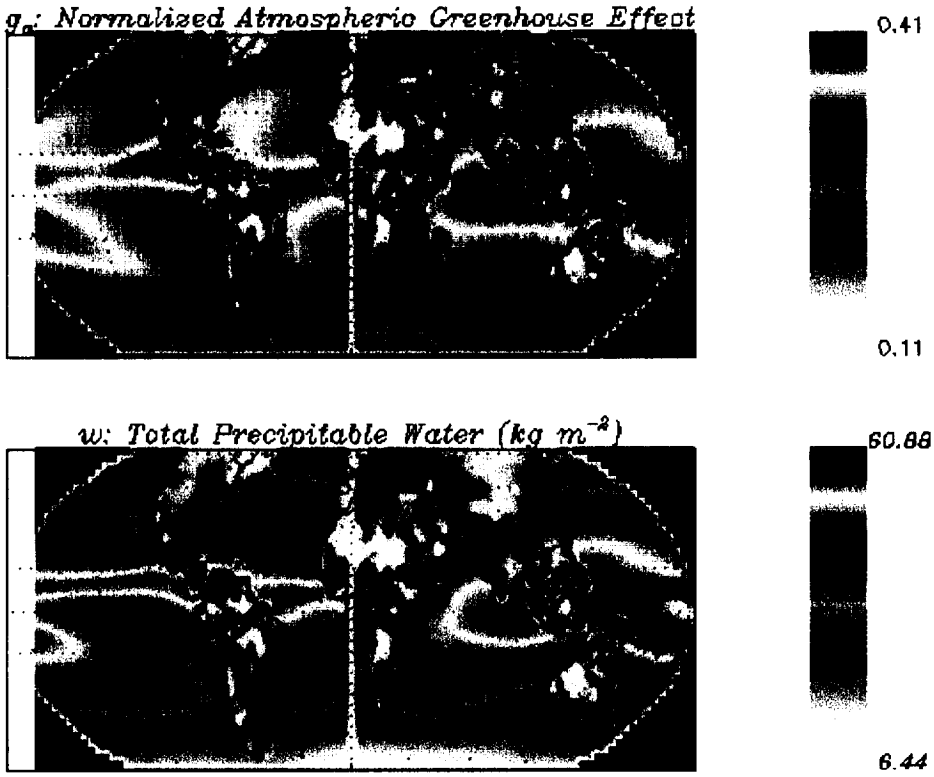

Fig. 4: Comparison between global observations of atmospheric greenhouse effect, g_a, (top panel) and total precipitable water vapor (lower panel). g_a is the reduction in the outgoing longwave radiation (OLR) due to the atmospheric greenhouse gases. It is derived from the difference between the OLR and the surface emitted radiation. The later is computed using correlative data of surface temperature and emissivity (40).

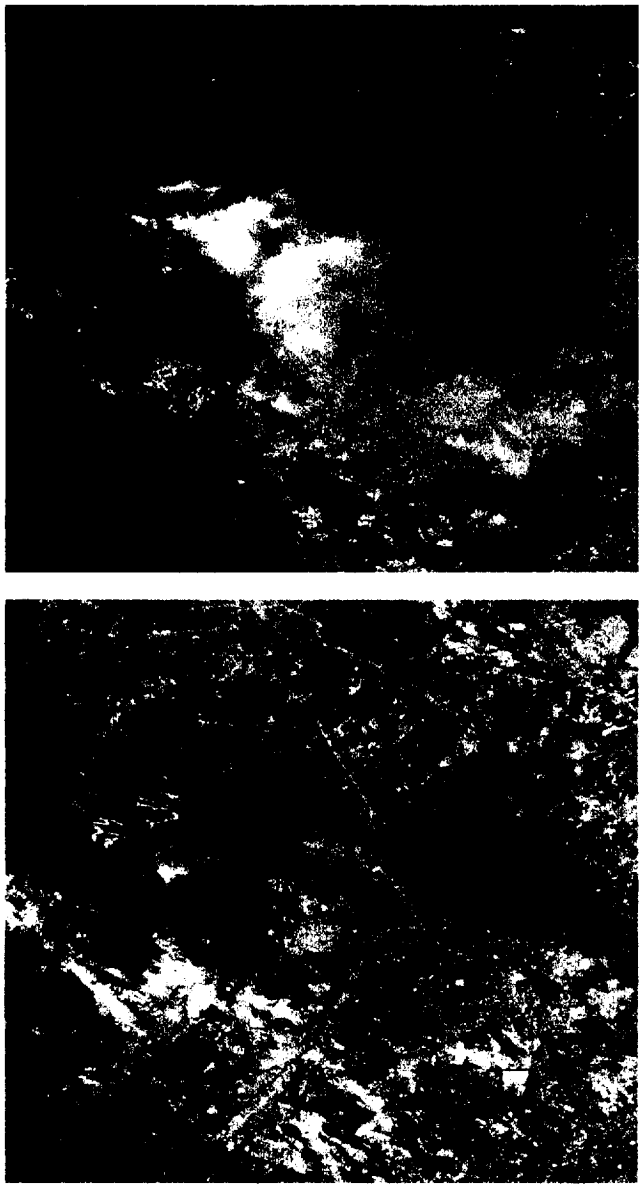

Fig. 5: Large fire near Cuiaba on Aug. 25, 1995 taken from the ER-2 AVIRIS instrument (identified by from Robert Green from JPL) during the SCAR-B experiment. The image is 10x20 km and 20 m resolution. Top image - heavy smoke emitted from the fire and flowing over Cuiaba. It resembles human vision and is composed of 0.47 μm (blue), 0.55 μm (green) and 0.66 μm (red). Bottom image - is for 2.1 μm (blue), 1.2 μm (green) and 1.65 μm (red). The smoke is almost transparent in these longer wavelengths and the fire is clearly seen with its 3 main temperatures zones (blue - glowing, purple - smoldering - emitting the heavy smoke, and white - the fire front). It is much easier to observe the surface features in the long wavelengths that penetrates the smoke. The solar zenith angle is 36°. The background optical thickness was 0.16 at 0.65 μm. The smoke optical thickness is on average higher by 0.6 from background, reflecting an additional 43 w/m^2 of solar radiation back to space.